Astron. Astrophys. 353, L25–L28 (2000)

ASTRONOMY AND ASTROPHYSICS

LETTER

Letter to the Editor

Multiple molecular outflows in AFGL 2688

P. Cox[1], R. Lucas[2], P.J. Huggins[3], T. Forveille[4], R. Bachiller[5], S. Guilloteau[2], J.P. Maillard[6], and A. Omont[6]

[1] Université de Paris XI, Institut d'Astrophysique Spatiale, Bât. 120, 91405 Orsay, France
[2] IRAM, 300 rue de la Piscine, 38406 Saint Martin d'Hères Cedex
[3] New York University, Physics Department, 4 Washington Place, New York, NY 10003, USA
[4] Observatoire de Grenoble, B.P. 53X, 38041 Grenoble Cedex, France
[5] IGN Observatorio Astronómico Nacional, Apt 1143, 28800 Alcalá de Henares, Spain
[6] Institut d'Astrophysique de Paris, CNRS, 98bis bd. Arago, 75014 Paris, France

Received 30 July 1999 / Accepted 12 October 1999

Abstract. We report high resolution ($1\farcs1 \times 0\farcs9$) imaging of the proto-planetary nebula AFGL 2688 in the CO (J=2–1) line and the continuum at 230 GHz, using the IRAM interferometer. The observations reveal with unprecedented detail the structure and the kinematics of the gas ejected by the star over the past few hundred years. Two distinct, high-velocity outflow directions are detected emerging from a central core of gas which surrounds the star: one is oriented north-south along the optical axis, the other is oriented east-west, close to the equatorial plane. We resolve the north-south and east-west outflows into a striking series of collimated, bipolar outflows. The tips of the outflows in the east-west direction correspond precisely to H_2 emission peaks seen in recent HST imaging at 2 μm, providing direct evidence for the impact and likely shaping effects of jets on the nearly spherical AGB molecular envelope. These outflows exemplify the mechanism by which point symmetries are imprinted on the structure of planetary nebulae at early stages of their formation.

Key words: ISM: planetary nebulae: general – ISM: planetary nebulae: individual: AFGL 2688 – ISM: molecules – stars: AGB and post-AGB

1. Introduction

The physical mechanisms which govern the evolution of proto-planetary nebulae (PPNe) are poorly documented because relatively few objects are known to be in this rapid transition between the AGB and planetary nebula phase (Kwok 1993). The role played by high-velocity winds which interact with the slowly expanding AGB envelope has been recognized as essential in the shaping of the planetary nebulae. However, the details of the interaction and the precise evolution from the symmetric AGB envelope to the asymmetries which characterize planetary nebulae are not well understood.

Send offprint requests to: P. Cox (cox@ias.fr)

AFGL 2688 (the 'Egg nebula') is one of the prime examples of a PPN which has evolved from the AGB phase about a hundred years ago (Jura & Kroto 1990). The nearly circular slowly expanding AGB envelope (with a diameter of about $20''$) is shocked by a warm, optically thin, fast wind (e.g., Young et al. 1992). Studies at high spatial resolution (e.g., Bieging & Nguyen-Quang-Rieu 1996) have shown that the bulk of the molecular gas is concentrated in the central $4''$ (or 6×10^{16} cm for an adopted distance of 1 kpc), coincident with the dark lane seen in optical images, with weaker extensions along the north-south axis. Observations at near-infrared wavelengths have revealed that high-velocity H_2 gas is present both in the north-south and east-west direction suggesting a quadrupolar outflow (Latter et al. 1993, Cox et al. 1997, Sahai et al. 1998).

In this letter, we present the results of a high angular resolution study of CO(2–1) emission which provide new insights into the structure and the kinematics of both the central regions and the high-velocity molecular gas in AFGL 2688.

2. Observations

The observations were made in the CO J=2–1 line and continuum at 230 GHz (1.3 mm) in January and March 1997 and March 1999 using the IRAM interferometer (Guilloteau et al. 1992) located at Plateau de Bure, France. The array consisted of five 15-meter antennas, equipped with SIS heterodyne receivers. The observations, centered on AFGL 2688, were made with three different configurations of the array (C, D and A). The primary beam is $22''$ (FWHM) at the frequency of the CO(2–1) line (the data presented are uncorrected for primary beam attenuation). The effective velocity resolution of the CO observations was 0.8 km s^{-1}. The observations of the continuum were also made with a bandwidth of 320 MHz. The radio-frequency passband and amplitude were calibrated using 3C273 (16 Jy at 230 GHz) and phase calibration was performed every 20 minutes using B2200+420 (1.4 Jy). The *u-v* data were Fourier-transformed and CLEANed, using the Clark algorithm. The restored Gaussian clean beam is $1\farcs07 \times 0\farcs85$ at a position angle of 70°. The

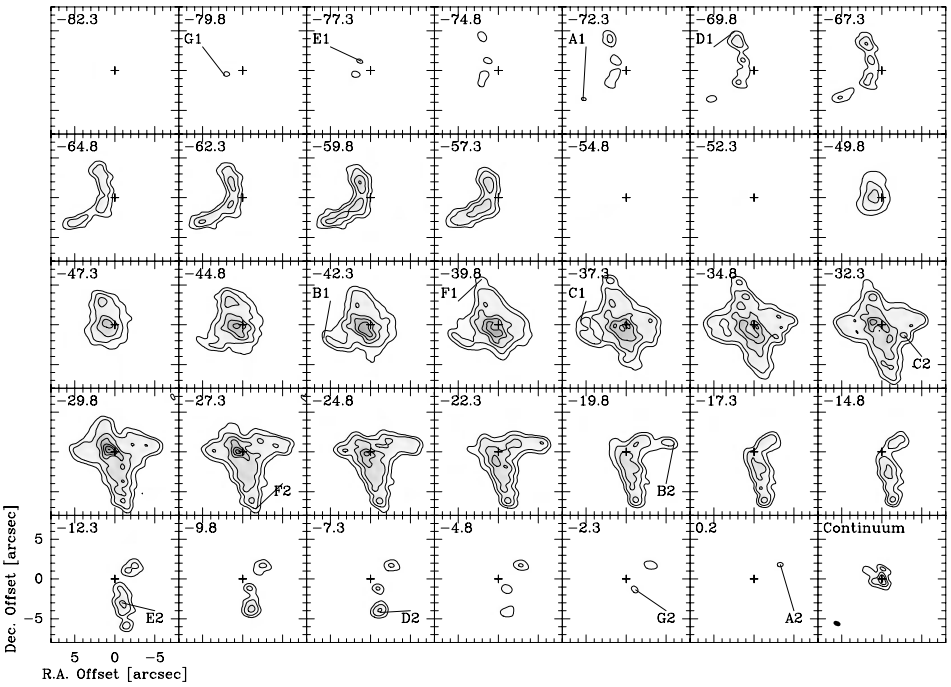

Fig. 1. Channel maps in the CO(2–1) line. The channel separation is $2.5\,\mathrm{km\,s^{-1}}$. The contours levels are 0.2, 0.5, and subsequent multiples of 0.5 Jy/beam. The coordinates of the map center are $\alpha = 21^{\mathrm{h}}02^{\mathrm{m}}18\overset{\mathrm{s}}{.}647$ $\delta = 36^{\circ}41'37\overset{''}{.}8$ (J2000.0) indicated by a cross. The synthesized beam ($1\overset{''}{.}07 \times 0\overset{''}{.}85$) is shown in the lower left corner of the continuum panel. The tips of the outflows are identified by letters A trough G in the relevant panels, labelled by LSR velocity.

continuum emission has been subtracted from the line channels. No correction has been made to recover the missing flux from extended structures. However, this will not affect the conclusions of this paper since most of the missing flux comes from the extended AGB envelope at velocities in the range (-50 to -20 $\mathrm{km\,s^{-1}}$), while most of the flux at high velocities is present in our map.

3. Results and discussion

The results of the observations are displayed in Fig. 1 as a series of channel maps together with the continuum at 1 mm. Fig. 2 presents a map of the velocity integrated CO emission compared to the HST image in the $H_2\ 1-0\,S(1)$ line emission and nearby 2.15 μm continuum (Sahai et al. 1998) for later discussion.

The CO and continuum observations shown in Figs. 1 and 2 provide a detailed picture of the distribution and kinematics of the gas recently ejected by the central star. Fig. 1 shows that the distribution of the CO emission is symmetric in both position and velocity with respect to the systemic velocity, $V_{\mathrm{sys}} = -34\,\mathrm{km\,s^{-1}}$(LSR). Note that in the velocity channels -50 to $-55\,\mathrm{km\,s^{-1}}$, the blue-shifted emission is completely absorbed by the approaching side of the AGB wind that lies between us and the central regions. At the systemic velocity, the CO emission consists of a central core $\sim 4''$ in diameter, with extensions in both the north-south and east-west directions. A similar structure is seen in the velocity integrated CO map in Fig. 2.

3.1. Multiple molecular outflows

At negative (approaching) velocities, the CO is detected in the northern and eastern extensions of the nebula (Fig. 1). The velocity behaviour along these structures is complex. Along the north extension, velocities increase away from the centre; the tip of the eastern arm is seen over a range of velocities from -60 to $-72\,\mathrm{km\,s^{-1}}$; and the highest velocity gas is found near the centre of the nebula up to $\sim -80\,\mathrm{km\,s^{-1}}$. At positive (receding) velocities, the CO gas is extended to the south and west, with a similar velocity structure to the blue-shifted gas, reversed about the systemic velocity (Fig. 1). The channel maps provide definite evidence of two distinct high-velocity outflow directions in AFGL 2688, one along a north-south axis at a P.A. of 17°, and the other in a roughly orthogonal direction east-west. Detailed examination of the CO data reveals that the two main outflows are resolved into a series of more collimated, bipolar outflows which are symmetric in direction and velocity about the center. The identification of the outflows is supported by the series of position-velocity diagrams along the main north-south axis and three east-west directions shown in Fig. 3. In the east-west direction, there are four outflows: the pairs A1/A2 and G1/G2 are detected at blue- and red-shifted velocities (about $\pm 25\,\mathrm{km\,s^{-1}}$from the systemic velocity), and the pairs B1/B2 (at $\pm 5\,\mathrm{km\,s^{-1}}$) and C1/C2 (at $\pm 2\,\mathrm{km\,s^{-1}}$) are traced at intermediate velocities [1] – see identifications in Figs. 2 and 3. It is striking that, for most of these outflows, the tips correspond precisely with the H_2 peaks seen in the HST image (Fig. 2). The only exceptions are in the central regions and to the west side of the equatorial plane, where the high-velocity red-shifted CO gas (located behind the dense central gas) has no clear H_2 counterpart in the HST image, most likely as a result of extinction in the near-infrared.

[1] Note that the peaks A1, B1, C1 and B2 correspond to the peaks E2, E3, E4, and E1, respectively, in the nomenclature of Sahai et al. (1998)

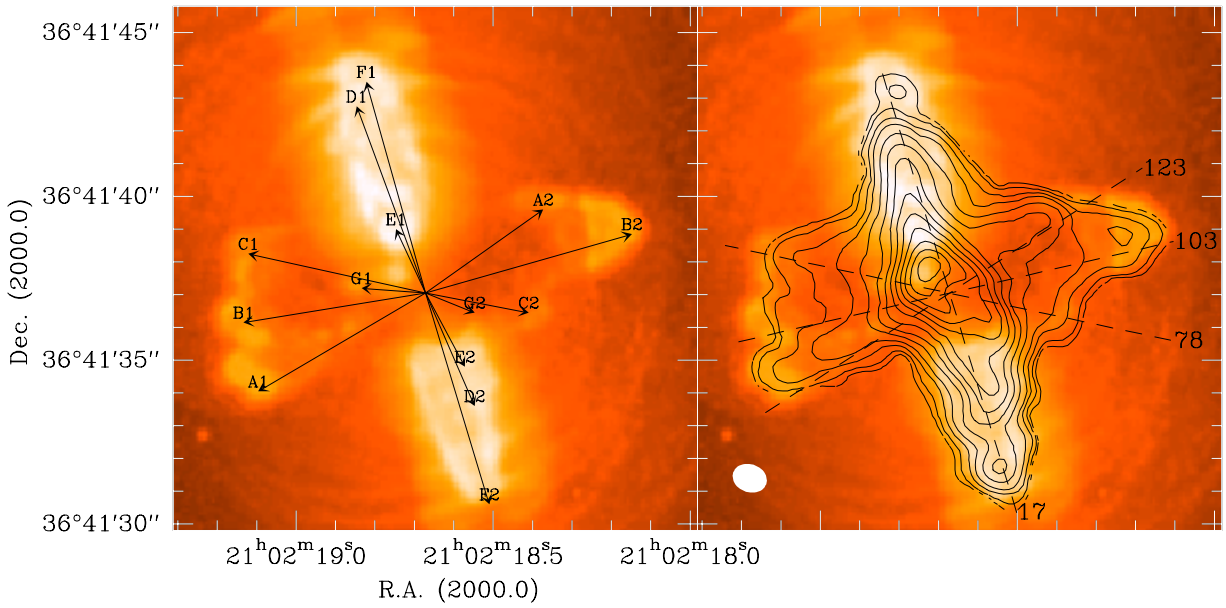

Fig. 2. The Plateau de Bure interferometer data compared to the H_2 1–0 S(1) line emission and nearby 2.15 μm continuum (in color) - from Sahai et al. (1998). The velocity integrated CO(2–1) emission is shown as contours (2, 4, 8, 12 to 72 by 6 Jy/beam) in the right panel, and the outflow axis are identified in the left panel (see also Fig. 1 and 3). The beam of the CO image is shown in the lower left corner of the right panel, with the locations of the position-velocity diagrams of Fig. 3

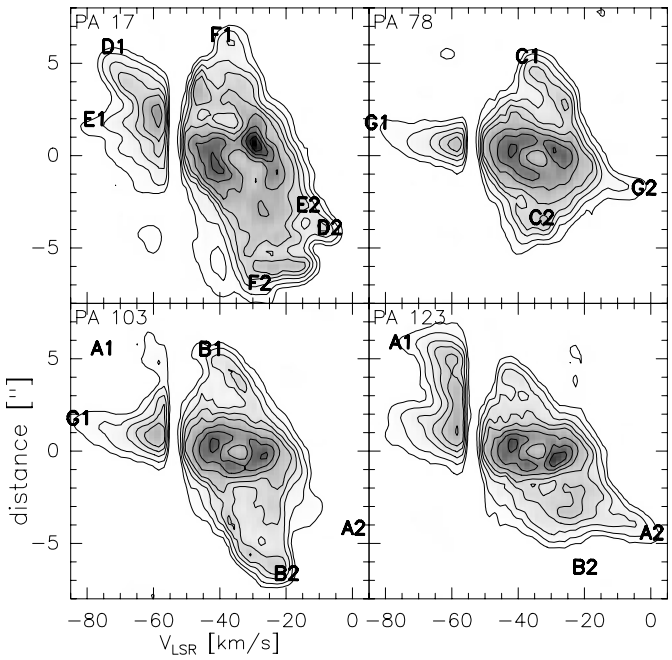

Fig. 3. Velocity-strip maps in the CO(2–1) line along the north-south bipolar outflow axis (P.A. 17°), and three east-west directions at P.A. of 78, 103, and 123° (see Fig. 2). The contours are 0.25, 0.5, 0.75, 1 to 2.6 by 0.4 Jy/beam. The extremities of the outflows are indicated.

In the north-south direction, three additional collimated outflows are detected (Fig. 3): D1/D2 and E1/E2 at the extreme red-shifted ($v < -18\,\mathrm{km\,s^{-1}}$) and blue-shifted ($v > -60\,\mathrm{km\,s^{-1}}$) velocities, and F1/F2 at intermediate ($\Delta v = \pm 6\,\mathrm{km\,s^{-1}}$) velocities, corresponding to the H_2 emission farthest from the center.

Along all the outflow axes (A to G), the CO velocity increases with distance from the centre. This implies that the observed CO gas is entrained by high-velocity jets which could be atomic or ionized. The velocity of the CO gas in the outflows is also higher by a factor of ∼2.5 than the velocity of the H_2 which is close to the expansion velocity of the AGB envelope (Kastner et al. 1999). The high-velocity jets entrain the CO gas and shock the molecular hydrogen of the AGB envelope. The lack of symmetry in the CO velocity between the east and west with respect to the systemic velocity could be due to inhomogeneities in the AGB envelope, or to destruction/creation of molecules in different regions of the shocks.

Assuming the model-dependent value of $i \sim 16°$ for the inclination of the north-south axis to the plane of the sky with the northern lobe towards the observer (Yusef-Zadeh et al. 1984), the deprojected flow velocity of F1 (at $6''$ from the centre) is $22\,\mathrm{km\,s^{-1}}$, corresponding to a kinematic age of ~ 1200 years. In comparison, the projected velocities of the jets D and E are $\sim 30\,\mathrm{km\,s^{-1}}$, implying ages of ∼250 and 125 years, if the same inclination is assumed. Finally, we note that the position of the central exciting star of AFGL 2688 recently derived from polarisation measurements (J. Kastner, private communication) lies within the positional errors at the intersection of the outflows (Fig. 2).

3.2. The core region

In addition to the collimated outflows, the present observations reveal in the central $2''$ a shell-like structure (Fig. 1) expanding with a velocity of at least $\sim 10\,\mathrm{km\,s^{-1}}$ (Fig. 3). This CO structure is not aligned with any of the outflow axes and lies at a P.A.

of $\sim 54°$, which is comparable to the direction of the 1.3 mm dust continuum emission (Fig. 1). The size of this structure ($1''$ or 1.5×10^{16} cm) implies that it was ejected ∼500 years ago (or less depending on the unknown inclination angle) and that it could trace the last episode of mass-loss on the AGB. We note that the expansion velocity of this structure is much slower than that of the envelope which expands rather at ~ 20 km s^{-1} (e.g., Young et al. 1992). Neither the distribution of the dense gas at the center nor its kinematics (Fig. 3) indicate the presence of an equatorial disk in AFGL 2688. The present data thus do not support the interpretation of a rotating equatorial disk to explain the east-west kinematics in AFGL 2688 (cf. Bieging & Nguyen-Quang-Rieu 1996, Kastner et al. 1999). Instead, the CO kinematics reveal the presence of a central expanding shell-like structure (not seen in H_2) and high-velocity gas with a morphology similar to the shocked H_2 gas tracing multiple, collimated outflows.

3.3. Origin and effects of the outflows

The presence of multiple, collimated outflows in two, roughly orthogonal directions cannot be explained by the standard two-winds model (e.g., Balick 1987). In this model, a fast spherical wind interacts with the slowly expanding AGB envelope and develops a bipolar outflow due to the presence of an equatorial density enhancement, commonly assumed to be the result of a close binary companion affecting the mass expelled by the AGB star (Morris 1987). Proto-planetary nebulae with morphologies similar to AFGL 2688 have recently been found (cf. Kwok et al. 1998, Su et al. 1998) and multipolar jets appear to be a common phenomenon in young planetary nebulae (e.g., Forveille et al. 1998, Sahai & Trauger 1998). Whatever the detailed processes involved are, the high-velocity winds must be intimately linked to the abrupt transition in the evolution of the star after the AGB phase. One important consequence of the jets is their shaping effect on the molecular envelope ejected on the AGB. The jets imprint complex point symmetries on the envelope, which later emerge as point symmetries seen in the ionized gas in the PN phase.

4. Conclusions

The observations reported here reveal the detailed structure and kinematics of the molecular outflows in AFGL 2688. A series of young (a few 100 years), high velocity, collimated outflows originate from the central star, and are directed along the north-south optical axis and in the east-west direction. The detailed correlation of the CO outflows with H_2 emission seen in AFGL 2688 provides direct evidence for their interaction with the nearly spherical envelope ejected on the AGB. These jets provide a mechanism by which complex point symmetries are imprinted on the envelopes and are seen in the later planetary nebula phase.

Acknowledgements. This work was supported in part by NSF grant AST-9617941 (to PJH).

We dedicate this Letter to the memory of five IRAM employees, Bernard Aubeuf, Francis Gillet, Henri Gontard, Roland Prayer, and Patrick Vibert, who lost their lives on July 1st, 1999, in a terrible teleferique accident, on their way to Plateau de Bure.

References

Balick B. 1987, AJ 94, 671
Bieging J.H., Nguyen-Quang-Rieu 1996, AJ 112, 706
Cox P., Maillard J.-P., Huggins P.J. et al. 1997, AA 321, 907
Forveille T., Huggins P.J., Bachiller R., Cox P. 1998 ApJ 495, L111
Guilloteau S., Delannoy J., et al. 1992, AA, 262, 624
Jura M., Kroto H. 1990 ApJ 351, 222
Kastner J.H., Henn L.A., Weintraub D.A., Gatley I. 1999, in *AGB Stars*, IAU Symp. 191, T. Le Bertre, A. Lebre, C. Waelkens (eds), ASP conf. series, p. 431
Kwok S. 1993, ARAA 31, 63
Kwok S., Su Y.L.S., Hrivnak B.J. 1998, ApJ 501, L117
Latter W.B., Hora J.L., Kelly D.M., Deutsch L.K., Maloney P.R. 1993, AJ 106, 260
Morris M. 1987, PASP 99, 1115
Sahai R., Hines, D.C., Kastner, J.H. et al. 1998, ApJ 492, L163
Sahai R., Trauger, J.T. 1998, AJ 116, 1357
Su K.Y.L., Volk K., Kwok S., Hvrinak B.J. 1998, ApJ 508, 744
Young K., Serabyn G., Phillips T.G., Knapp G.R., Güsten R., Schultz A. 1992, ApJ 385, 265
Yusef-Zadeh F., Morris M., White R.L. 1984, ApJ 278, 186